Geophys. J. Int. (2008) doi: 10.1111/j.1365-246X.2008.03805.x

Land subsidence pattern controlled by old alpine basement faults in the Kashmar Valley, northeast Iran: results from InSAR and levelling

Jan Anderssohn,[1] Hans-Ulrich Wetzel,[1] Thomas R. Walter,[1] Mahdi Motagh,[1,2] Yahya Djamour[3] and Hermann Kaufmann[1]

[1] *GeoForschungsZentrum Potsdam,* D-14473 *Potsdam, Germany. E-mail: calypso@gfz-potsdam.de*
[2] *Department of Geomatics and Surveying Engineering, University of Tehran, Iran*
[3] *National Cartographic Center of Iran, Teheran, Iran*

Accepted 2008 March 30. Received 2008 March 17; in original form 2007 July 6

SUMMARY

Fluid storage systems, such as oil, gas, magma or water reservoirs, are often controlled by the host rock structure and faulted terrain. In sedimentary basins, where no direct information about underlying structure is available, the pattern of ground deformation may allow us to assess the buried fault arrangement. We provide an example in the semi-arid area of Iran, in the Kashmar Valley, a region subject to land subsidence due to water overexploitation. Geodetically determined subsidence rates in the Kashmar Valley exceed 15–30 cm yr^{-1}. The pattern of surface deformation is strongly non-uniform and displays NE–SW elongated bowls of subsidence. The trend resembles old Cretaceous-to-Tertiary faults that evolved during early alpine tectonic deformation. Although these early alpine structures are considered tectonically inactive in the present day, the observed land subsidence pattern indicates significant structural control on the geometry of the aquifer basin and its deformation during reservoir drainage.

Key words: Spatial analysis; Radar interferometry; Hydrology; Tectonics and climate interactions; Fractures and faults; Asia.

INTRODUCTION

Groundwater reservoirs in arid and semi-arid regions are limited and often subject to intense and uncontrolled groundwater extraction. In the Middle East, about 5 per cent of the world's population has to share less than 1 per cent of available freshwater, so water has become a major economic and strategic resource (Oren 2002). Since arid and semi-arid regions cover more than 60 per cent of Iran, the lack of water may hinder further spread of agricultural and economic activities (Modarres & de Paulo Rodrigues da Silva 2007). Many of the water reservoirs in the Middle East are deep-rock aquifers of Cretaceous or even Triassic origin, with expected recharge times in the order of thousands of years (Beaumont *et al.* 1988). In Iran, intense irrigation associated with land use is thought to be the main reason for groundwater overdrafting and a measurable shrinkage of the water reservoirs. The amount of groundwater extraction in the country has increased from 20 billion m^3 in 1960 to more than 53 billion m^3 in 2002–2003, exceeding safe yields. In addition, the available water resource per capita shrank from 5800 m^3 in 1965 to about 1910 m^3 in 2001, and is estimated to be less than 1000 m^3 in 2025 (World Bank 2005).

Intensive water extraction can compact the aquifer system, increasing the effective overburden intergranular load. As a result, the land may subside. If the reservoir recharge is less than the discharge, compaction and land subsidence can become irreversible (Sneed *et al.* 2003) and may affect agricultural and urban areas that are heavily dependent on groundwater supplies (Poland 1984). In addition, associated land subsidence can cause significant damage to infrastructure. Annual costs of water degradation in Iran (mean estimate, 2002) approach US $3.2 billion or 2.82 per cent of the Gross Domestic Product, of which about 10 per cent is related to damage costs associated with aquifer exploitation (World Bank 2005).

Currently there are no reliable estimates for the rate and extent of land subsidence in the groundwater basins of Iran. Several studies have used the remote sensing method Interferometric Synthetic Aperture Radar (InSAR) for monitoring of groundwater-induced land subsidence (Galloway *et al.* 1998; Amelung *et al.* 1999; Galloway *et al.* 2000b; Lu & Danskin 2001; Hoffmann *et al.* 2003; Motagh *et al.* 2007). Compared to conventional techniques for monitoring land deformation (GPS, levelling), the main advantage of InSAR is its ability to provide high resolution (a few tens of metres) maps of crustal deformation with large spatial coverage ($>10^4$ km) at subcentimetre accuracy (Bürgmann *et al.* 2000; Hansen 2001).

In this study, we investigate land subsidence in the Kashmar region, a valley in northeastern Iran approximately 220 km south of the province's capital, Mashhad (Fig. 1). We shall use InSAR data to measure groundwater-induced deformation in Kashmar and compare the results with precise levelling. These observations allow us to examine in detail the spatio-temporal pattern of subsidence that can be used to infer underlying structural conditions. In the following we first describe the issue of water overextraction in the study area. Then, we outline the methods used to measure the associated effects. Finally, we compare the observed subsidence pattern to the tectonic framework of the region.

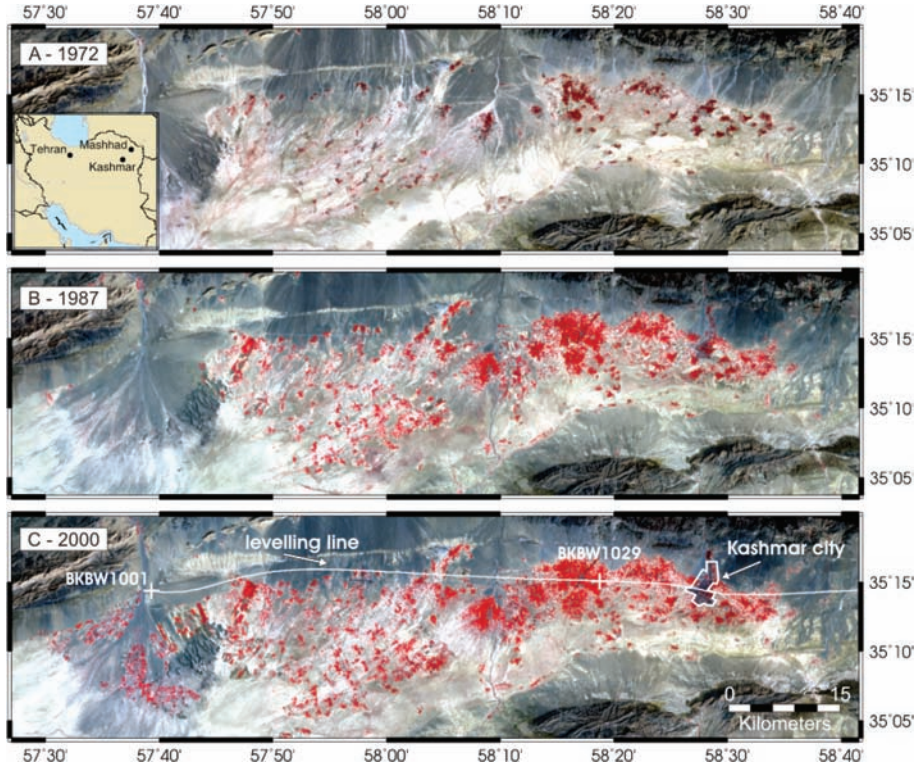

Figure 1. Landsat MSS, TM and ETM+ colour composite image maps at different times: (A) 1972 October, (B) 1987 August and (C) 2000 September. The red pixels depict vital vegetation. Due to early and ongoing data acquisition of Landsat satellites, a significant increase in vegetation in Kashmar Valley was found for the past 35 yr. The white line in (C) displays the location of the first-order precise levelling line. Buildings and streets appear grey.

KASHMAR VALLEY

The Kashmar topographic basin is oriented in an approximately east–west direction and is about 100 km long and as much as 25 km wide (Fig. 1). The city of Kashmar is located at the eastern end of the valley, with a population between 70 000 and 180 000. In recent decades, Kashmar Valley has been known for its commercialized growth of grapes, cultivation of pistachio and production of raisins. The colour composite maps in Fig. 1 show an increase in agriculture in the valley defined by three Landsat scenes taken in 1972, 1987 and 2000. The development of Kashmar city can also be seen by an increase in the overall footprint of the city. The figures of increased agriculture and urban development suggest an increasing water demand. After 2000 no suitable Landsat data are available for further assessment of the recent changes in agriculture. However, analysis of ENVISAT's MERIS (Medium Resolution Spectrometer) multispectral measurements still show a slight increase in the vegetation cover of the spring season (inset in Fig. 2a), as defined by the change in the value of normalized difference vegetation index (NDVI) (Tucker 1979). The increasing demand in water is also reflected in the ground water level data. Groundwater level measurements of several piezometric wells in Kashmar Valley show a groundwater level decline by about 12 m from 1988 to 2004 (Fig. 2a). Using a linear regression, we estimate an annual groundwater level decline of about 70 cm yr^{-1} in the Kashmar area. A comparison of the groundwater level decline to precipitation data suggests that climate change has only a minor influence. The precipitation archive at the Kashmar synoptic station (http://www.irimo.ir) suggests a large variance but may imply a slight decrease of about 57 mm yr^{-1} in the annual precipitation rate from 1998 to 2006 and a mean temperature increase of about 1.3 °C within this period (Fig. 2b). Therefore, a combination of the growing use of intensive agriculture in the valley since 1972, the prospering city, the increased temperature and the slight net decrease in annual precipitation rate may explain the increased demand for groundwater. As we will show below, the effects of increased water extraction may include substantial land displacement controlled by basement structures, which can be indirectly inferred by remotely sensed satellite data.

METHODS

As the first method to investigate land subsidence we use radar data from the ENVISAT satellite in image mode (I2) that has a ground resolution of approximately 20 m, a scene size of about 100 × 100 km^2, a fixed incidence angle of about 23°, and a revisit interval of 35 d. We used a total of 22 SAR Single Look Complex (SLC) images for the time interval from July 2003 to March 2006 at the descending satellite track 435. We utilize the 2-pass InSAR method (Massonet and Feigl 1998) implemented in the software package SARscape (www.sarmap.ch), with the 90 m resolution digital elevation model (DEM) generated by the NASA Shuttle Radar Topography Mission (SRTM) to remove the topographic phase contribution from the interferometric phase. Twenty-two interferograms with favourable baselines and temporal coverage (Fig. 3) are processed and unwrapped using the region growing algorithm (Reigber & Moreira 1997). InSAR coherence is good in the study area for time spans over a few months. For time spans exceeding ∼200 d, however, we lose coherence probably because of intensive agriculture in the valley. Ground deformation, measured by C-band InSAR (wavelength ∼56 mm), is generally visualized in fringes (colour

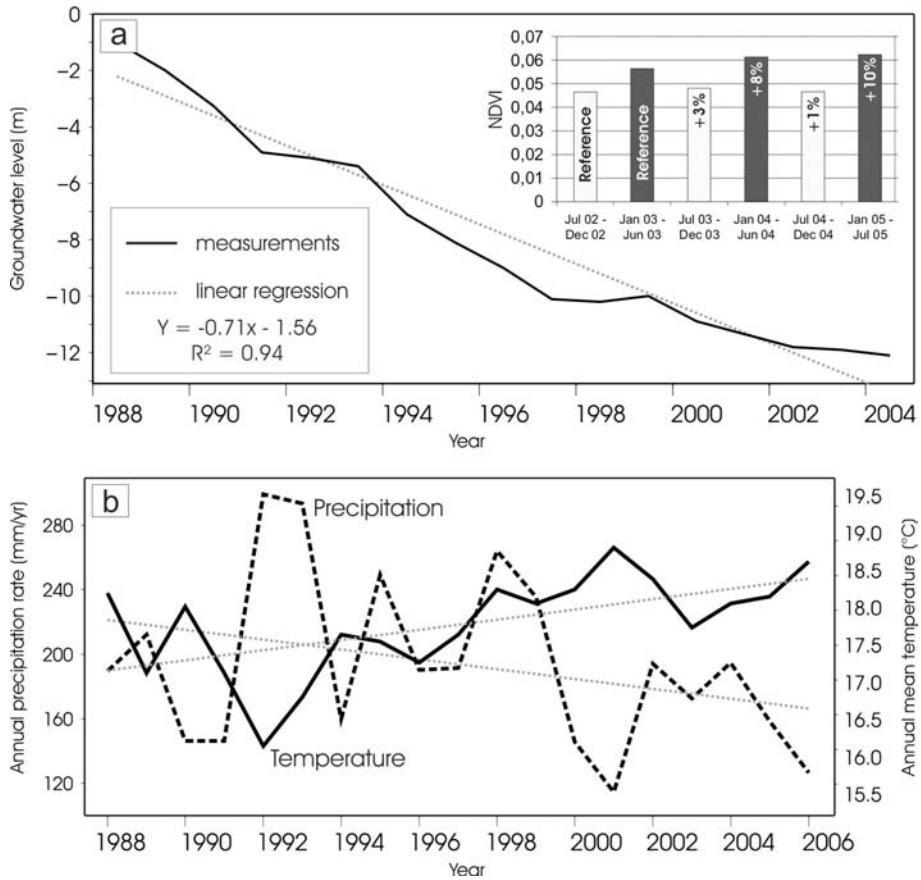

Figure 2. (a) Plot of groundwater level at piezometric wells located in the subsidence area. Shown here is the average value of several piezometric wells and a linear regression line (dashed). A decline of groundwater level by approximately 71 cm yr^{-1} was estimated for these stations for the period 1988–2004. Inset displays a diagram of half a year averaged NDVI values based on 37 monthly MERIS level-2b data sets. A slightly trending increase in NDVI was observed over 3 yr for the spring covering season. (b) Annual mean temperature and precipitation values between 1988 and 2006. Temperature increased by about 1.3 °C, while precipitation decreased by about 60 mm between 1988 and 2006, assuming a linear regression (dashed lines).

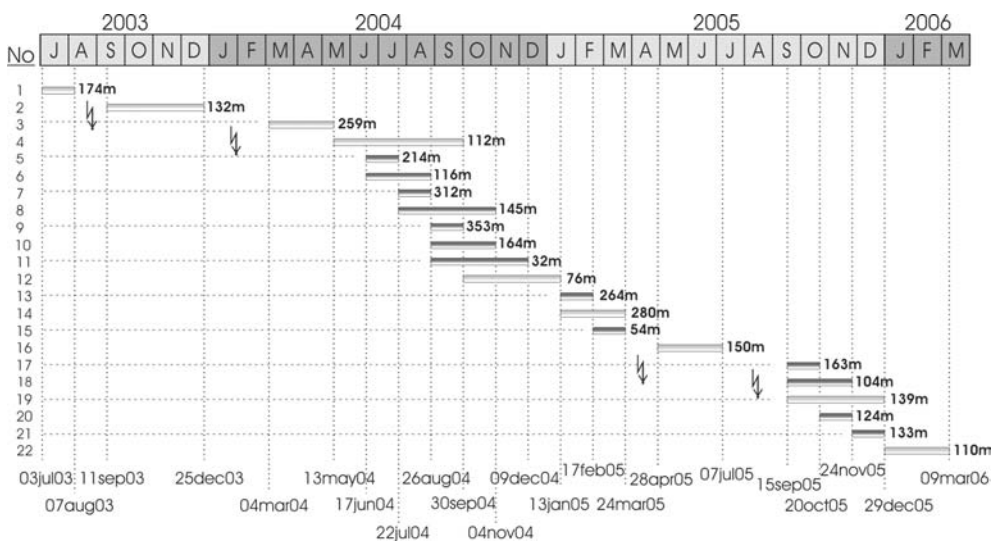

Figure 3. Overview of all 22 interferograms processed (satellite track 435). The headline bar represents the time scale, given by the number of years and months as letters. The accurate timing of master and slave images is shown on the bottom. Horizontal bars represent the interferograms and normal baselines are depicted on their right-hand sides. Red flashes indicate data gaps. Light grey filled bars represent interferograms used for consecutive time-series.

cycles), each fringe representing a displacement of 2.8 cm in the line-of-sight (LOS) of the satellite. For the satellite's incidence angle of 23°, one fringe can be converted into a vertical displacement of 3.1 cm, assuming that the LOS range changes are dominated by vertical deformation alone. The perpendicular baseline of the interferograms ranges from 32 to 353 m, which involves height ambiguity (height differences corresponding to an interferometric fringe) of about 230 and 21 m, respectively. The relative height error

(90 per cent probability) of SRTM elevation data over Eurasia is ∼8.7 m (Rodríguez *et al.* 2005), resulting in no more than ∼0.4 fringes, or 0.14 cm, of line-of-sight error in the interferogram with the longest perpendicular baseline. Moreover, the basin floor is very flat that helps mitigate any contributions from topography-related artefacts in interferograms. An overview of the data that are processed here along with their acquisition dates and normal baselines is shown in Fig. 3. Other interferograms not included in this study have either poor coherence or unfavourable baselines. Using all suitable data we analysed the spatio-temporal evolution of subsidence in Kashmar Valley.

In order to validate the results of space-borne remote sensing data, the InSAR measurements are compared to independent ground truth observations obtained using levelling. The National Cartographic Center of Iran (NCC) collected levelling data in the Kashmar Valley over a 10-yr time span between 1993 and 2003. The first survey was done during 1993 August–October and the second survey from May to July in 2003. Fig. 1(c) shows the location of the levelling line along the Kashmar Valley. The levelling surveys were conducted according to specifications required for first-order precise levelling; the expected standard deviation for the change in elevation differences between two benchmarks as measured in two surveys can be expressed as $\pm\alpha L^{1/2}$, where $\alpha = 1$ mm km$^{-1/2}$ and L is the distance in kilometres along the levelling line between the benchmarks (Memarzadeh 1998).

RESULTS

Fig. 4 shows a sample wrapped interferogram, superimposed on the corresponding SAR amplitude image, with one fringe representing ∼2.8 cm of displacement in satellite line-of-sight. It covers the period from 2005 April 28 to July 7, and shows up to 6 cm of land subsidence. The subsidence area extends ∼65 km from east to west and ∼12 km from north to south, including an area of ∼750–800 km^2 in the valley. The main subsidence feature is elongated along the axis of the valley and appears to be related to its flat plains, flanked by mountainous areas to the north and south. The regions surrounding Kashmar Valley do not show any significant signs of surface deformation and consequently are considered stable. Some local phase gradients outside of the subsidence zone may be due to residual topographic or atmospheric noise.

Comparing various interferograms covering different time periods allows us to examine the spatial extension, temporal evolution and amount of land subsidence in greater detail. Fig. 5 presents

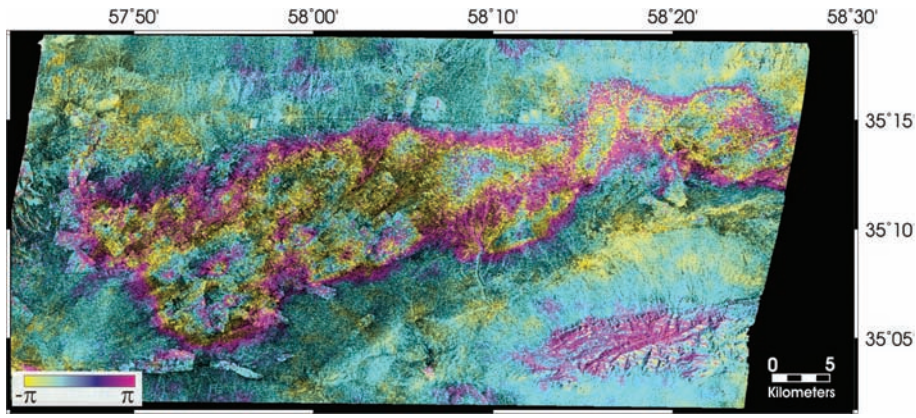

Figure 4. SAR differential interferogram of land-surface deformation over Kashmar Valley, Iran, during the period 2005 April 28, to 2005 July 7 (interferogram No. 16 in Fig. 3) superimposed on a corresponding amplitude image. Each full colour cycle (fringe) represents subsidence of 2.8 cm in line-of-sight of the satellite. Local heterogeneities of differing subsidence behaviour are clearly visible. One fringe for the valley and additional fringes for the local heterogeneities can be found, yielding subsidence of about 3 cm for Kashmar Valley and more than 6 cm for local heterogeneities.

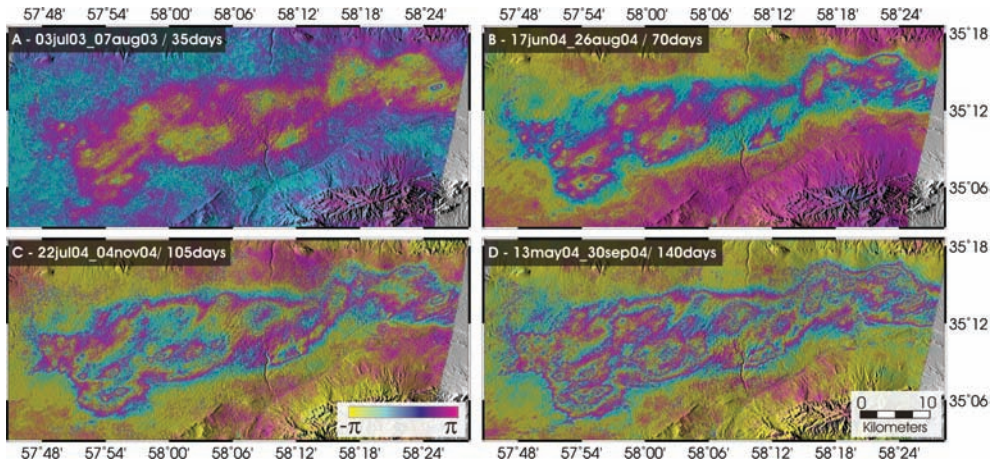

Figure 5. Four examples of wrapped interferograms with time spans (A – 35, B – 70, C – 105 and D – 140 d). The evolution of the subsidence distribution pattern with increasing time is evident in these four interferograms, showing that the amount of displacement increases with time while the general location appears to be constant.

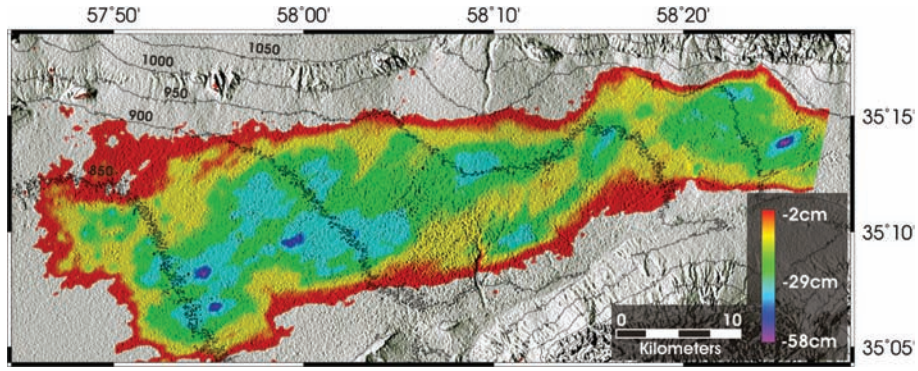

Figure 6. Cumulative (∼2 yr) displacement map resulting from a consecutive time-series of interferograms, also shown with elevation contour lines. An established pattern of subsidence distribution is visible, indicated by local bowls and widespread homogenous subsidence. A maximum subsidence of about 58 cm is obtained at local bowls, whereas most of the area (60 per cent) is affected by subsidence up to 30 cm.

four wrapped interferograms overlain on the corresponding shaded relief map. These interferograms have time spans of 35, 70, 105 and 140 d, respectively, and reveal that the amount of subsidence increases over longer time periods, as indicated by the rising numbers of fringes, while its spatial pattern remains approximately constant over time. The area affected by subsidence is about 750–800 km^2 in all interferograms, and the boundaries of the subsiding area are well defined. These boundaries are only roughly correlated with topography. The amount of subsidence is generally larger in the centre of the valley, and displays isolated and aligned subsidence bowls trending NE–SW.

To estimate the cumulative subsidence that occurred between 2003 July and 2006 March, we add nine interferograms that cover consecutive acquisition dates. Light grey bars in Fig. 3 highlight these interferograms. Some 60 per cent of the area affected is subject to subsidence of about 15 cm yr^{-1}. As shown in the displacement map (Fig. 6), several isolated locations subsided by as much as 58 cm for the integrated time (2.1 yr). The pattern of subsidence in the displacement map is similar to the pattern obtained in individual interferograms. There are widespread subsidence bowls that are spatially elongated in a NE–SW direction with localized areas of more pronounced subsidence inside them.

To validate this pattern we also stack all 22 interferograms to amplify the signal to noise ratio and estimate the rate of subsidence, assuming a constant rate. The average monthly subsidence rate reaches up to ∼2.5 cm month^{-1} for the integrated time from 2003 July 3 to 2006 March 9 (Fig. 7). The velocities obtained from the stacked InSAR data by 22 interferogams (Fig. 7) and by nine consecutive interferograms (Fig. 6) provide a distinct correlation, confirming the assumption of constant subsidence rate.

Fig. 8 shows the comparison between the InSAR-stack results and levelling measurements along an east–west line (see Fig. 1c). The relative errors of levelling data are indicated on the profile as error bars, ranging between 1.3 and 9.6 mm; these quantities apply for the original measurements (time span 9.75 yr). The standard deviation converted into annual values is accordingly smaller. For the InSAR-stack along the levelling line, error propagation resulted in 1.4 mm standard deviation, considering a measured LOS standard deviation of about 0.3 cm outside the subsidence-affected area. The comparable standard deviations of InSAR and levelling results permit a quantitative comparison between them.

From 1993 to 2003, the largest subsidence along the levelling profile occurs east of the Kashmar City, where it amounts to ∼1.2 m at the benchmark BKBW1029, or a rate about 11 cm yr^{-1} (Fig. 1c). Significant subsidence has only affected the agricultural part of Kashmar Valley. Both levelling and InSAR-stack transects show a steep gradient in subsidence area with little subsidence outside the agriculture area (see Fig. 1c). The InSAR-stack transect captures more local vertical deformation, due to the finer resolution of InSAR (∼20 m) with respect to the levelling (∼2 km). The near zero subsidence values west of longitude 58°12′ observed by both InSAR and levelling suggest that the InSAR results do not have a constant offset and that the boundaries of subsidence area have remained constant. East of longitude 58°12′, the amount of subsidence per year is larger for the InSAR-stack result. This may suggest that the rate of subsidence has increased since at least 2003 within the affected area.

DISCUSSION

We have applied the InSAR method for data acquired between 2003 and 2006 to determine the extent and amount of subsidence in Kashmar Valley. Approximately 750–800 km^2 in this valley is subsiding at decimetre rates annually. For short-term interferograms (e.g. 35 d separation), our results suggest that the subsidence rate is constant. However, comparison of long-term and short-term interferograms (e.g. 140 d) shows small changes for some very localized maxima of subsidence, probably resulting from varying amount of groundwater pumped and seasonal weather changes.

The stack of interferograms shows a subsidence pattern similar to the individual interferograms (Fig. 5). The rates of subsidence observed in both the levelling and InSAR-stack data agree well. Based on the agreement of trends and the small differences in amplitude between levelling and the InSAR-stack, we presume that the spatial extent of the subsidence area is constant, while its amplitude has slightly increased since at least 2003 (the start date of InSAR data). This is in part supported by the overall decrease in annual precipitation, the temperature increase and continued overdrafting of groundwater over the past years (Fig. 2), contributing to more subsidence.

InSAR also reveals a distinct pattern of subsidence, which may be influenced, if not controlled, by buried tectonic structures within and below the young sediments infilling the valley. The detailed analysis of subsidence in the Kashmar depression reveals isolated regions of maximal subsidence, as well as NE–SW elongated zones of subsidence bowls (Fig. 7). This complex subsidence pattern may indicate the influence of buried fault block structure within and below the aquifer-bearing sedimentary basin fill. The

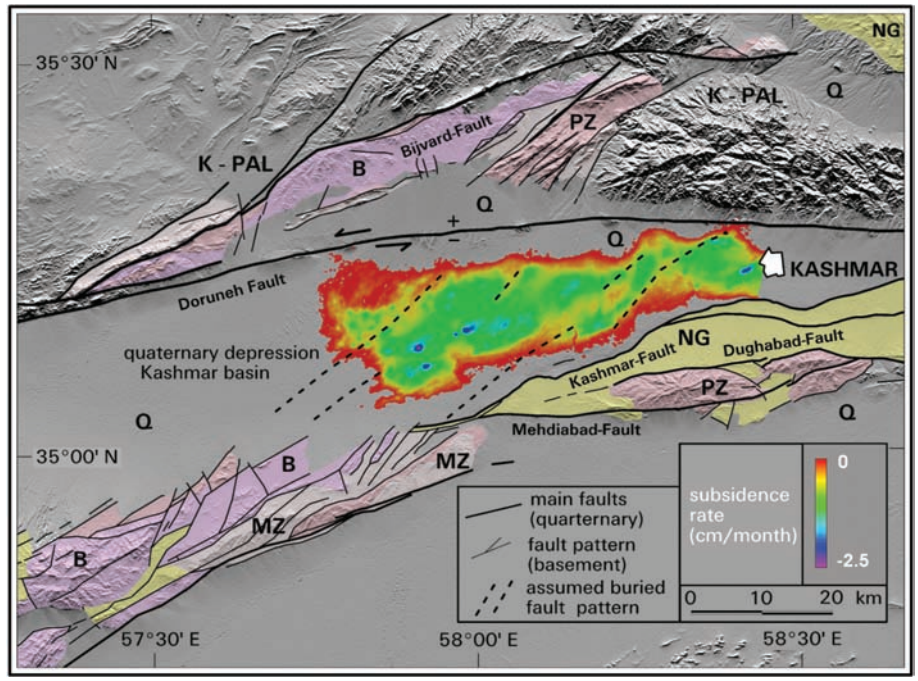

Figure 7. Monthly subsidence rate map overlain on a shaded relief map containing geological features. Note that the subsidence pattern on a regional scale is controlled by the Quaternary depression, and on a local scale by bowls striking parallel to buried Mesozoic faults. B – basement (Precambrian or early Paleozoic metamorphics), PZ – Paleozoic to Middle Triassic metamorphics; MZ – folded Mesozoic units, mainly Jurassic to Lower Cretaceous sandstones and conglomerates, shales, limestones, K-PAL – Upper Cretaceous – Paleogene sequence, (volcanics, granites, evaporates and clastics), NG – faulted Neogene clastics and red bed sediments; Q – Quaternary depressions, filled with gravel fans, salt flats, dunes and Neogene clastics; Seismically active fault zones are Bijvard, Doruneh (sinistral strike-slip fault with relative upthrown) and Kashmar, Mehdiabad and Dughabad (thrust faults). These features are mapped based on a Landsat ETM+ scene and SRTM DEM and are supported by the 1:250 000 geological map published by the Ministry of Industry and Mines Geological Survey of Iran (mosaic of Feredows, Gonsabad, Kashmar and Torbat sheets) and a map of major active faults in Iran from the International Institute of Earthquake Engineering and Seismology (IESS).

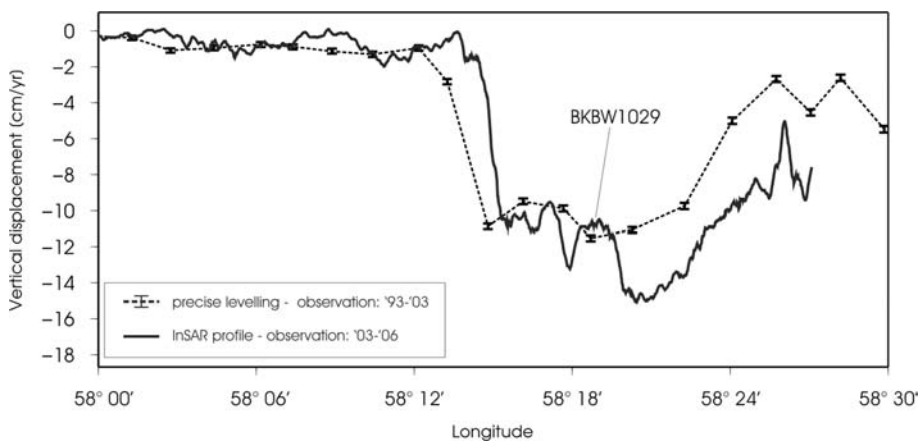

Figure 8. Result of first-order precise levelling surveys in Kashmar Valley between 1993 and 2003 (see Fig. 1c for location of benchmarks) and the results of the InSAR data. The changes in geodetic levelling are divided by the time span (9.75 yr) to find the subsidence rate in centimetres per year. The InSAR transect relies on the stack of interferograms and is also converted by dividing by the integrated time span to subsidence rate per year. Error bars in the levelling profile represent standard deviations in cumulative random errors from the reference benchmark.

subsidence-affected area is part of the tectonically controlled Quaternary basin structure, evolved from several Alpine deformation steps of the Central Iranian Plateau (e.g. Guest *et al.* 2007). In this process, the sinistral Doruhneh fault (Mohajer-Ashjai 1975), Berberian & Tchalenko 1976) forms the northern boundary of the Lut Block and the Kashmar depression, including the subsidence area. Its southern boundary is controlled by recent thrust systems related to the Kashmar, Doughabad and Mehdiabad faults. The folding and source mechanisms of earthquakes in the 1970s (Mohajer-Ashjai 1975) suggest NE–SW compression corresponds to the left-lateral movement of the Doruhneh fault and the development of NW–SE dilatation elements. Contemporaneously, this geodynamic model would enable the development of NE–SW directed graben (fault) structures in the affected Kashmar depression. The

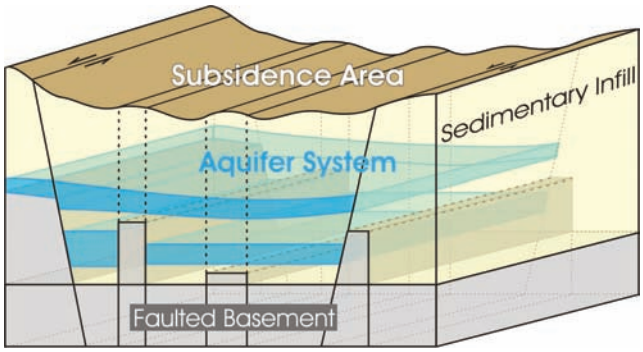

Figure 9. Sketch of suggested subsidence model. The extensive subsidence distribution pattern at the surface is mainly controlled by Quaternary faults cutting through the basin fill and the pumped aquifer system sediments.

outcropping NE–SW striking morphological and tectonic block structures of the basement in the north and south of the subsidence area suggest the continuation of similar block or graben structures within and below the basin-filling sedimentary and aquifer units. Sediments of varying thickness and an aquifer system displaying irregular water recharge rates overlie this buried faulted basement structure that propagates through the basin fill deposits. The situation is sketched in Fig. 9, hypothesising that heavy pumping in localized subsidence zones is producing elongated subsidence patterns that are directly fault controlled.

Other studies suggest comparable structural control of subsidence pattern, as for instance in the Silver Creek region of California (Galloway and Hoffmann 2006), Las Vegas (Bell *et al.* 2002) or Mashhad (Motagh *et al.* 2007). The characteristic of these presented boundaries suggest differing sedimentary sections of contrasting mechanical or dynamic properties, and faults cutting the pumped aquifers serving as subsidence barriers (Galloway *et al.* 2000a).

Considering the water level decline of about 71 cm and the 15–30 cm subsidence per year, we infer highly compressible sediments in the aquifer system. The lithology of Kashmar Valley is mainly characterized by low level and young piedmont fan and valley terrace deposits. We cannot decipher whether the locations of areas affected by maximum subsidence are located (1) above faults or (2) between faults in the basement and sediment fill. In case (1), the fault may host large reservoirs, which have been drained and are leading to more subsidence in zones elongated along NE–SW. In case (2), the fault may cause replenishment of the reservoirs and thus be associated with less subsidence, as sketched in Fig. 9.

The aquifer system may therefore be highly heterogeneous with varying skeletal storage coefficient (Hoffmann *et al.* 2001). Due to the lack of contemporaneous measurements of water levels in the vicinity of the areas affected by more subsidence, a quantitative evaluation of the skeleton coefficient is not feasible. Special dedicated field observations in the future may help to develop reliable models and assess the extraction-induced compaction and subsidence.

CONCLUSION

Our analysis shows subsidence in the east–west elongated Kashmar Valley in northeast Iran. During the study period 2003–2006, subsidence affected an area of about 750–800 km^2, with common subsidence rate of 15 cm yr^{-1}. At several isolated locations, however, the rates are even up to twofold larger, reaching almost 30 cm yr^{-1}. We also observe that these locations probably correlate to technical buildings and well locations.

Zones of widespread subsidence bowls, which are punctuated by very localized maxima, are generally elongated NE–SW along the axis of the valley. We suggest that the NE–SW elongated subsidence pattern is governed, if not controlled, by old buried faults of Cretaceous-to-Tertiary age beneath or within the sedimentary valley infill. Buried faults may accordingly form a structured aquifer basin system varying in thickness and recharge rate.

Taking into account the ongoing and increased subsidence inferred by levelling and measured by InSAR, the increased demand for groundwater caused by increasing agriculture, global climate change and precipitation decline, we expect that the overexploitation of groundwater in Kashmar (Fig. 2) is likely to become a major factor for development and prosperity in this region.

ACKNOWLEDGMENTS

We would like to thank the National Cartographic Center of Iran for providing levelling data and supporting our work. We also thank Mrs S. Chabrillat and N. Richter for advice concerning imaging spectrometry. The paper benefited from constructive comments by J.W. Bell and an anonymous reviewer. ENVISAT-ASAR, -MERIS data were provided by the European Space Agency under Category-1 research proposal No. 3188 and 2892. M. Motagh gratefully acknowledges financial support from the German Research Foundation (MO 1851/1–1).

REFERENCES

Amelung, F., Galloway, D., Bell, J., Zebker, H. & Laczniak, R.G., 1999. Sensing the ups and downs of Las Vegas: InSAR reveals structural control of land subsidence and aquifer-system deformation, *Geology,* **27,** 483–486.

Beaumont, P., Blake, G.H. & Wagstaff J.M., 1988. *The Middle East: A Geographical Study,* pp. 624, David Fulton, London.

Bell, J., Amelung, F., Alan, R. & Geoff, B., 2002, Land subsidences in Las Vegas, Nevada, 1935–2000: new geodetic data show evolution, revised spatial patterns, and reduced rates, *Environ. Eng. Geosci.,* VIII, 155–174

Berberian, M. & Tchalenko, J., 1976. Bibliography with abstracts on the seismicity and tectonics of Iran, *Geol. Surv. Iran,* **39,** 429–516.

Bürgmann, R., Rosen, P.A. & Fielding, E.J., 2000. Synthetic aperture radar interferometry to measure earth's surface topography and its deformation, *Ann. Rev. Earth planet. Sci.,* **28,** 169–209.

Galloway, D.L. & Hoffmann, J., 2006. The application of satellite differential SAR interferometry-derived ground displacements in hydrogeology. *Hydrogeol. J.,* **15,** 133–154.

Galloway, D.L., Hudnut, K.W., Ingebritsen, S.E., Phillips, S.P., Peltzer, G., Rogez, F. & Rosen, P.A., 1998. Detection of aquifer system compaction and land subsidence using interferometric synthetic aperture radar, Antelope Valley, Mojave Desert, California, *Wat. Res. Res.,* **34,** 2573–2585.

Galloway, D., Bürgmann, R., Fielding, E., Amelung, F. & Laczniak, R. 2000a. Mapping recoverable aquifer-system deformation and land subsidence in Santa Clara Valley, California, USA, using space-borne synthetic aperture radar, in *Proceedings of the 6th International Symposium on Land Subsidence, Ravenna, Italy, 24–29 Sept 2000 National Research Council of Italy (CNR),* Vol. 2, pp. 229–236.

Galloway, D., Jones, D. & Ingebritsen, S., 2000b. Measuring land subsidence from space, *Geological Survey Fact Sheet*-051–00.

Guest, B., Guest, A. & Axen, G., 2007. Late Tertiary tectonic evolution of northern Iran: a case for simple crustal folding, *Global planet. Change,* **58,** 435–453.

Hanssen, R.F., 2001. *Radar Interferometry: Data Interpretation and Error Analysis,* Vol. 2, pp. 308, Kluwer Academic Publishers, Dordrecht, The Netherlands.

Hoffmann, J., Zebker, H., Galloway, D. & Amelung, F., 2001. Seasonal subsidence and rebound in Las Vegas Valley, Nevada, observed by synthetic aperture radar interferometry, *Water Res. Res.,* **37,** 1551–1566.

Hoffmann, J., Galloway, D.L. & Zebker, H.A., 2003. Inverse modeling of interbed storage parameters using land subsidence observations, Antelope Valley, California, *Wat. Res. Res.,* **39,** SBH5-1–SBH5-13.

Lu, Z. & Danskin, W.R., 2001. InSAR analysis of natural recharge to define structure of a ground-water basin, San Bernadino, California, *Geophys. Res. Lett.,* **28,** 2661–2664.

Massonnet, D. & Feigl, K.L., 1998. Radar interferometry and its application to changes in the earth's surface, *Rev. Geophys.,* **36,** 441–500.

Memarzadeh, Y., 1998. Refraction effect and statistical analysis of the Iran first order precise levelling data, *Master thesis*. K.N. Toosi University of Technology, Iran.

Modarres, R. & de Paulo Rodrigues da Silva, V., 2007. Rainfall trends in arid and semi-arid regions of Iran, *J. Arid Environ.,* **70,** 344–355.

Mohajer-Ashjai, A., 1975. *Recent and Contemporary Crustal Deformation in Eastern Iran,* Imperial College London, London.

Motagh, M., Djamour, Y., Walter, T.R., Wetzel, H., Zschau, J. & Arabi, S., 2007. Land subsidence in Mashhad Valley, northeast Iran: results from InSAR, levelling and GPS, *Geophys. J. Int.,* **168,** 518–526.

Oren, Michael B., 2002. *Six Days of War: June 1967and the Making of the Modern Middle East,* pp. 480, Oxford University Press Inc., New York.

Poland, J., 1984. *Guidebook to Studies of Land Subsidence Due to Ground-Water Withdrawal,* pp. 305, UNESCO Studies and Reports in Hydrology, Paris, France.

Reigber, A. & Moreira, J., 1997. Phase unwrapping by fusion of local and global methods, in *Proceedings of the IGARSS'97,* pp. 869–871, Singapore, 3–8 August 1997.

Rodríguez, E., Morris, C., Belz, J., Chapin, E., Martin, J., Daffer, W. & Hensley, S., 2005. *An Assessment of the SRTM Topographic Products,* pp. 143, Technical Report JPL D-31639, Jet Propulsion Laboratory, Pasadena.

Sneed, M., Ikehara, M.E., Stork, S.V., Amelung, F. & Galloway, D.L., 2003. *Detection and Measurement of Land Subsidence Using Interferometric Synthetic Aperture Radar and Global Positioning System, San Bernardino County, Mojave Desert, California,* U.S. GEOLOGICAL SURVEY, Water-Resources Investigations Report 03-4015.

Tucker, C.J., 1979. Red and photographic infrared linear combinations for monitoring vegetation, *Remote Sens. Environ.,* **8,** 127–150.

World Bank, 2005. *Islamic Republic of Iran: Cost Assessment of Environmental Degradation,* Report No. 32043-IR, Washington, DC.